Voltage-Dependent Blockade of Connexin40 Gap Junctions by Spermine

Hassan Musa and Richard D. Veenstra
Department of Pharmacology, SUNY Upstate Medical University, Syracuse, New York 13210

ABSTRACT The effects of spermine and spermidine, endogenous polyamines that block many forms of ion channels, were investigated in homotypic connexin (Cx)-40 gap junctions expressed in N2A cells. Spermine blocked up to 95% of I_j through homotypic Cx40 gap junctions in a concentration- and transjunctional voltage (V_j)-dependent manner. V_j was varied from 5 to 50 mV in 5-mV steps and the dissociation constants (K_m) were determined from spermine concentrations ranging from 10 μM to 2 mM. The K_m values ranged from 4.9 mM to 107 μM for $8.6 \leq V_j \leq 37.7$ mV, within the physiological range of intracellular spermine for $V_j \geq 20$ mV. The K_m values for spermidine were ≥ 5 mM. Estimates of the electrical distance (δ) for spermine ($z = +4$) and spermidine ($z = +3$) were 0.96 and 0.76 respectively. Cx40 single channel conductance was 129 pS in the presence of 2-mM spermine and channel open probability was significantly reduced in a V_j-dependent manner. Similar concentrations of spermine did not block I_j through homotypic Cx43 gap junctions, indicating that spermine selectively blocks Cx40 gap junctions. This is contrary to our previous findings that large tetraalkylammonium ions, also known to block several forms of ion channels, block junctional currents (I_j) through homotypic connexin Cx40 and Cx43 gap junctions.

INTRODUCTION

The connexin (Cx) family of proteins, of which there are over 16 mammalian isoforms, form an intercellular plasmalemmal channel that mediates the exchange of soluble molecules between adjacent cells according to their electrical and chemical gradients (Goodenough et al., 1996; Beyer and Willecke, 2000). Each gap junction channel is formed by a dodecamer of protein subunits, a hexamer of connexin molecules in each of two adjacent plasmamembranes that align in an end-to-end manner to form the complete channel (Makowski et al., 1977). The two hexameric hemichannels of a gap junction channel have a cytoplasmic opening of ~40 Å that narrows within the membrane to 12–15 Å and widens again within the extracellular space to 25 Å (Perkins et al, 1997; Unger et al., 1999). This central pore exhibits modest charge and molecular selectivity of less than ten-to-one for potassium over chloride and fluorescent tracer molecules of less than 900 Da, depending on homomeric and heteromeric connexin composition (Imanaga et al., 1987; Veenstra et al., 1995; Elfgang et al., 1995; Trexler et al., 1996; Beblo and Veenstra, 1997; Wang and Veenstra, 1997). The four transmembrane α-helices and two extracellular loops of the connexins possess the highest degree of amino acid homology while the cytoplasmic loop and carboxyl-terminus exhibit the least homology (Beyer et al., 1990). Despite the known conserved membrane topology and three-dimensional resolution to 7 Å, it is not known which cytoplasmic, transmembrane, and extracellular domains of the connexin molecule form the permeation pathway for ions and other solutes. Site-directed and substituted cysteine mutagenesis studies suggest that the amino terminus (NT), first transmembrane domain (M1), and first extracellular loop (E1) potentially line a portion of the pore in each respective compartment (Verselis et al., 1994; Zhou et al., 1997; Trexler et al., 2000).

Voltage-dependent block of ion channels, characteristic of association between the blocking ion and the channel protein partially within the transmembrane voltage field, was crucial to the identification of pore-forming domains of several forms of K^+ channels (Woodhull, 1973; French and Shoukimas, 1985; Yellen, 1987; MacKinnon and Yellen, 1990). Recently, we employed this approach with the tetraalkylammonium series of organic cations that block potassium and many other types of ion channels (Musa et al., 2001). Unfortunately, tetrapentylammonium (TPeA) and tetrahexylammonium (THxA) ions were poorly permeant and did not permit an exact determination of an electrical distance to the site of block within the permeation pathway of Cx40 gap junctions. The polyamines, particularly spermine and spermidine, are ubiquitous aliphatic amines that regulate neuronal toxicity and excitability by interactions with calcium-permeable glutamate receptor channels and cardiac excitability by modulation of inward rectification in inward rectifier K^+ (IRK) channels (Scott et al., 1993; Nichols et al., 1996; Ruppersberg, 2000). Spermine and spermidine produce the intrinsic rectification of the IRK channels by blocking the pore in a voltage-dependent manner (Ficker et al., 1994; Lopatin et al, 1994, 1995). A single acidic residue was identified as the site of polyamine block within the IRK channel that was also identified as the site of ionic block by Cs^+ and Rb^+ (Wible et al., 1994; Abrams et al., 1996). The polyamines are rapidly being shown to block several other types of ion channels as well (Williams, 1997).

Cx40 and Cx43 are the predominant connexins expressed in the myocardium and ventricular conduction system of the

Submitted February 15, 2002, and accepted for publication August 26, 2002.

Address reprint requests to Richard D. Veenstra, Ph.D., Dept. of Pharmacology, SUNY Upstate Medical University, 750 East Adams Street, Syracuse, NY 13210. Tel.: 315-464-5145; Fax: 315-464-8014; E-mail: veenstrr@upstate.edu.

0006-3495/03/01/205/15 $2.00

mammalian heart. We examined the effects of spermine and spermidine on homotypic Cx40 and Cx43 gap junctions by measuring the junctional conductance (g_j) in the presence of 10 μM to 15 mM unilateral polyamine concentrations. Both polyamines blocked Cx40 g_j in a concentration- and V_j-dependent manner. The site of block by spermine and spermidine senses 96% and 76% of the V_j field respectively. Conversely, the same concentrations of spermine did not block Cx43 g_j. These results provide the first demonstration of an impermeant block of a gap junction channel that discriminates between the two predominant myocardial gap junction proteins, Cx40 and Cx43.

MATERIALS AND METHODS

Electrophysiological recording

Stable rCx40 transfected neuro2A (N2A) cell cultures were prepared and maintained as previously described (Beblo et al., 1995). N2A cell cultures were washed 3–5 times with HEPES-buffered saline immediately before use and placed on the stage of an inverted phase contrast microscope (Olympus IMT-2, Lake Success, NY). The bath saline contained (in mM): 142 NaCl, 1.3 KCl, 0.8 $MgSO_4$, 0.9 NaH_2PO_4, 1.8 $CaCl_2$, 4.0 CsCl, 2.0 TEACl, 5.5 dextrose, 10 HEPES, pH 7.4 (titrated with 1N NaOH), 310 mosm. All junctional current (I_j) recordings were performed using conventional double whole cell recording techniques using two Axopatch 1D (Axon Instruments, Foster City, CA) patch clamp amplifiers (Veenstra, 2001). Patch electrodes (PG52151-4, WPI, Inc., Sarasota, FL) had tip resistances of 4–6 MΩ before GΩ seal formation and patch break when filled with 140 mM KCl internal pipette solution (IPS). The standard KCl IPS contained (in mM): 140 KCl, 4.0 CsCl, 2.0 TEACl, 3.0 $CaCl_2$, 5.0 K_4BAPTA, 1.0 $MgCl_2$, 25 HEPES, pH 7.4 (titrated with 1N KOH), 310 mosm. MgATP was added daily to achieve a final concentration of 3.0 mM. Polyamine salts were added unilaterally as indicated for each experiment. Spermine HCl and Spermidine HCl (Calbiochem, La Jolla, CA) were stored as a 500-mM stock solution in 18 MΩ-cm water and diluted as required with KCl IPS. The final osmolarity of the polyamine + KCl IPS was not adjusted because the maximum dose of 15-mM spermidine altered the final IPS volume by 1% and the total osmolarity by 9%. For most polyamine concentrations [PA], the IPS osmolarity was altered by $\approx$3%. All experiments were performed at room temperature (20–22°C). Off line current and voltage data recordings were stored on VCR tape using a Neurocorder DR-484 2/4 channel digitizer (Cygnus Technology, Delaware Water Gap, PA) at 10 kHz direct from the patch clamp amplifier. All analyzed currents were digitized at 2 kHz and low pass filtered at 100 Hz (WPI LPF-30) unless otherwise indicated. Analysis was performed using pClamp version 8.0 (Axon Intruments, Inc.) or the DOSTAT analysis program in the case of single gap junction channel currents (Manivannan et al., 1992). Final graphs and curve fitting were performed using Kaleidagraph version 3.5 (Synergy Software, Reading, PA) or Origin version 6.1 (OriginLab Corporation, Northampton, MA) software.

To determine the magnitude of polyamine block, a voltage protocol was written that sequentially altered the holding potential (ΔV_1) of the PAHCl + KCl-containing cell (cell 1) from negative to positive and back to negative potentials relative to the KCl-containing cell (cell 2) in 30-s intervals. The common holding potential (V_1 and V_2) was −40 mV for both cells. Cell 1 was stepped to this common potential for 10 s between different −/+/− command voltage sequences to assess any change in the nonjunctional voltage clamp circuit. $V_j = (V_1 + \Delta V_1) - V_2$ and ΔV_1 was altered in 5-mV increments from 5 to 50 mV and $I_j = -\Delta I_2$. One example of the I_j recordings obtained from an experiment with 2-mM spermine at $V_j = -/+/-40$ mV is shown in Fig. 1. There were no time-dependent changes in I_j observed during the control V_j pulse to −40 mV. Appreciable time-dependent decay and recovery of I_j was observed during the first 5 s of the subsequent block and recovery +/−40 mV V_j pulses in all polyamine experiments. I_j was averaged over the last 15 s of each 30-s V_j pulse (Fig. 2 *A*) to determine the steady state I_j and junctional I-V relationships were plotted for every experiment as shown in Fig. 2 *B*. This plot demonstrates the reversibility of the polyamine-dependent block using this voltage protocol. The maximum junctional conductance ($g_{j,max}$) was calculated from the slope of the linear regression fit of the −5 to −25 mV I_j-V_j curve for each experiment. All V_j values were corrected for junctional series resistance errors using quantitative methods to correct for whole cell patch electrode values during g_j measurements according to the following expression:

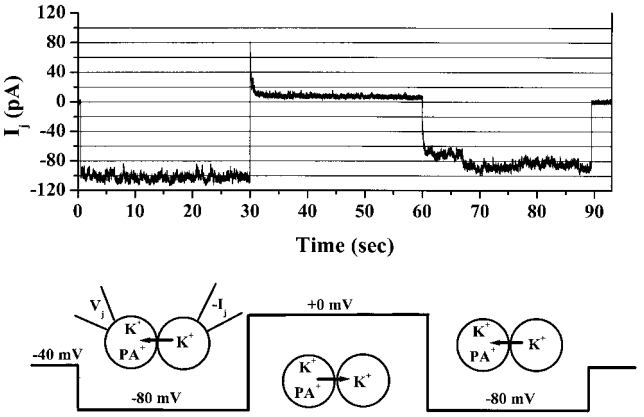

FIGURE 1 Voltage protocol for the determination of polyamine block of Cx40 junctional current (I_j). The baseline adjusted junctional currents ($-\Delta I_2 = I_j$, see Eq. 1) from the postjunctional cell (2) of a rat Cx40-transfected N2A cell pair in the presence of 2-mM spermine in the prejunctional cell (1) are shown (*upper panel*) for a transjunctional voltage (V_j) sequence of −/+/−40 mV. Displayed is a single sequence of an entire protocol in which V_j was varied in 5-mV increments from ±10 to ±50 mV. The V_j polarity is in reference to the prejunctional cell (cell 1). For each V_j, cell 1 was stepped from a common holding potential of −40 mV ($V_j = 0$) to a negative command potential (negative V_j, control), to a voltage step of equal amplitude but opposite polarity (positive V_j, block), and finally returning to the control voltage for 30 s each (recovery). Each −/+/− (control/block/recovery) voltage sequence was followed by a 10-s rest period (V_j = 0 mV). The direction of net cationic flux, that drives the polyvalent spermine cation into the pore, is indicated in the illustration (*lower panel*).

$$g_j = \frac{-\Delta I_2}{V_1 - (I_1 \times R_{el1}) - V_2 + (I_2 \times R_{el2})} \quad (1)$$

(Veenstra, 2001).

RESULTS

Effects of unilateral polyamines on junctional current-voltage relationships

Varying concentrations of spermine were added unilaterally to the patch pipette of cell 1 in a rat Cx40-transfected N2A cell pair. Experimental concentrations of spermine ranged from 10 μM to 2 mM. In the presence of 2-mM spermine, the junctional I-V relationship exhibits rectification indicative of V_j-dependent blockade of Cx40 I_j beginning at +10 mV that achieves maximum block ($\cong$95%) above +30 mV (Fig. 2 *A*).

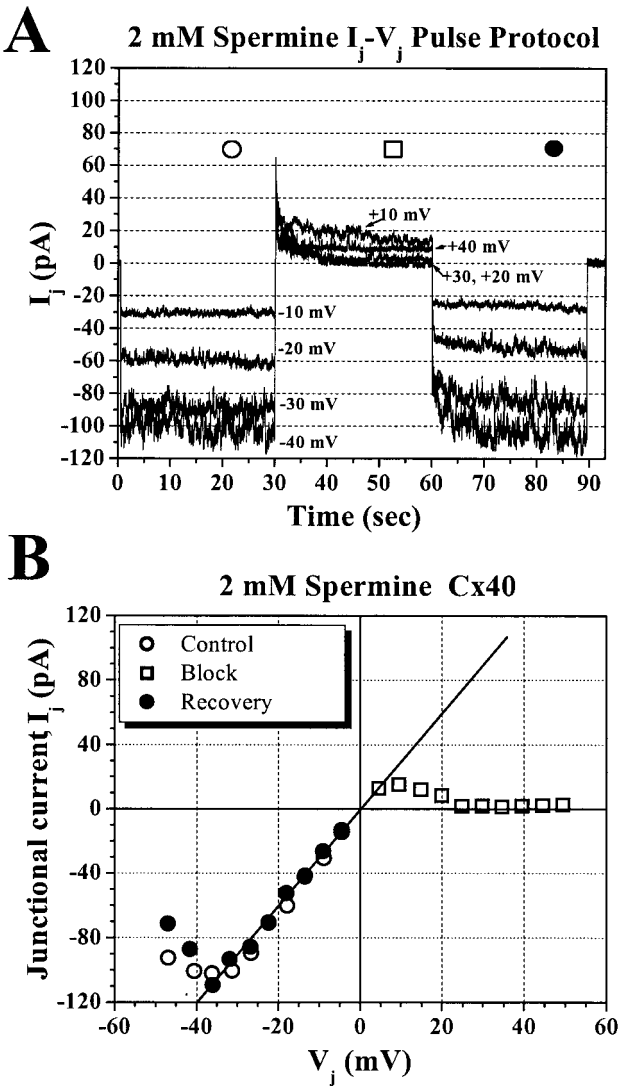

FIGURE 2 Reversible block of Cx40 I_j by 2-mM spermine. (*A*) Junctional current records elicited by 10, 20, 30, and 40 mV sequences demonstrating the voltage- and time-dependent block by 2-mM spermine. The steady-state control (○), block (□), and recovery (●) junctional currents were averaged over the last 15 s of each V_j step. (*B*) The complete steady-state junctional current–voltage (I–V) relationship for the 2-mM spermine experiment shown in panel A. The reversibility of the block by 2-mM spermine at positive V_j values is demonstrated by the similarity of the control and recovery I_j-V_j curves.

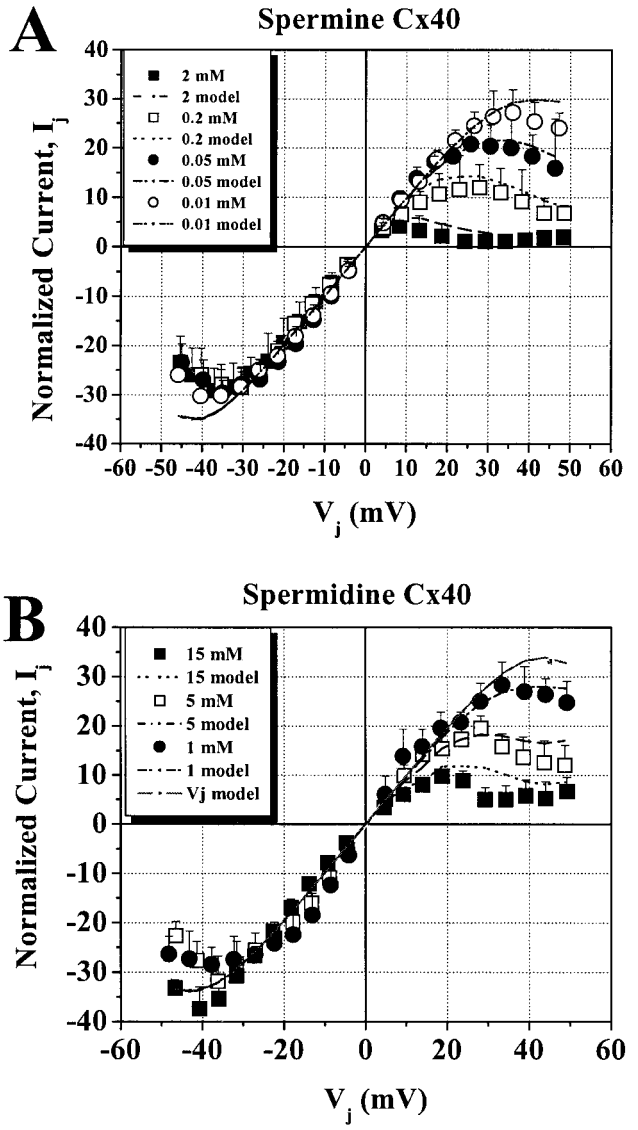

FIGURE 3 Concentration-dependent polyamine junctional I–V curves. (*A*) Normalized steady-state junctional I_j-V_j relationships for 10 μM, 50 μM, 200 μM, and 2 mM spermine added unilaterally to cell 1. All I_j-V_j curves were normalized to their linear slope g_j obtained between V_j values of -5 to -25 mV (linear range of g_j) and the normalized junctional I–Vs were pooled for each spermine concentration. Each data point represents the mean ±SD for each V_j value. The solid line is the predicted junctional I–V relationship for Cx40 gap junctions using Eq. 2 to model the V_j-dependence of the normalized junctional conductance (G_j) as previously determined (Veenstra, 2001, see text for details). The four different dashed lines indicated in the legend predict the additional effect of V_j-dependent block by 10 μM, 50 μM, 200 μM, and 2 mM spermine on rCx40 I_j as calculated by Eq. 3. The $K_m(V_j)$ values for spermine are provided in Table 1. Ionic block is evident at spermine concentrations >0.01 mM. (*B*) Normalized steady-state junctional I_j-V_j relationships for 1 mM, 5 mM, and 15 mM spermidine added unilaterally to cell 1. Each data point represents the mean ±SD for each V_j value. The solid line again illustrates the V_j-dependence of G_j for rCx40 according to Eq. 2. The dashed lines predict the junctional I–V relationship according to Eq. 3 using the $K_m(V_j)$ values for spermidine provided in Table 1. The normalized junctional I–V relationships were pooled for each spermidine concentration as described for spermine. Ionic block is evident at spermidine concentrations >1 mM.

The complete steady state I_j-V_j relationship for this experiment is shown in Fig. 2 *B*. This I_j-V_j curve demonstrates near complete blockade (□) of Cx40 I_j at $V_j \geq +25$ mV that is fully reversible depending upon V_j polarity. The control (○) and recovery (●) I_j values are shown at all negative V_j values in this example.

The mean junctional I–V relationships for four spermine concentrations are shown in Fig. 3 *A*. The junctional I–V relationships were normalized to their $g_{j,max}$ as described in the Materials and Methods and pooled for each experimental

concentration. The normalized junctional current-voltage curves are of the form $I_j = (g_j/g_{j,max}) \times V_j$. The $g_{j,max}$ varied between 1–12 nS and the overall average g_j was 5.15 ± 2.81 nS. The mean g_j (± SD) values were 5.89 ± 2.95 nS ($n = 5$), 5.29 ± 4.58 nS ($n = 7$), 4.94 ± 1.62 nS ($n = 6$), 6.46 ± 1.91 nS ($n = 5$), 5.02 ± 3.29 nS ($n = 8$), 4.89 ± 3.97 nS ($n = 7$), 4.80 ± 1.75 nS ($n = 3$), 4.84 ± 3.50 nS ($n = 7$), and 4.22 ± 1.75 nS ($n = 7$) for 10 μM, 20 μM, 50 μM, 100 μM, 200 μM, 350 μM, 500 μM, 1 mM, and 2 mM spermine, respectively.

The intrinsic V_j-dependent gating of Cx40 was observed above ±40 in all experiments. The regulation of steady-state G_j for Cx40 as illustrated by the solid line was calculated using the following expression:

$$I_{j,ss} = V_j \cdot \left[\frac{G_{j,max} \times [\exp(A \cdot (V_j - V_{1/2}))] + G_{j,min}}{1 + [\exp(A \times (V_j - V_{1/2}))]}\right], \quad (2)$$

where $G_{j,max} = 1$ ($G_j = g_j/g_{j,max}$ = normalized slope conductance for each experiment), $G_{j,min}$ = the minimum value of $g_j/g_{j,max}$, A = the slope factor for the Boltzmann curve = zF/RT, and $V_{1/2}$ = the half-inactivation voltage. The slope factor is proportional to the gating charge movement (z) of the state transition. For Cx40, $G_{j,min} = 0.26$, $V_{1/2} =$ 50 mV (−50 mV for negative V_j values), and $A = -0.15$ (+0.15 for negative V_j values) for a net gating charge of 3.8 elementary charges as described by Veenstra (2001).

A reduction in I_j was apparent only at positive V_j values (holding potentials positive to −40 mV in the spermine-containing cell) and increased with increasing spermine concentration and V_j. Only the 10 μM, 50 μM, 200 μM, and 2 mM junctional I-V curves are shown in Fig. 3 *A*. The predicted junctional I-V curves based on the V_j-dependent dissociation constants ($K_m(V_j)$) for spermine block (see Table 1 for the $K_m(V_j)$ values) and the intrinsic V_j-gating of g_j are also illustrated. The steady-state junctional I–V curves were calculated by the following equation:

$$I_{j,ss} = V_j \times \left[\frac{1}{1 + ([PA]/K_m(V_j))}\right] \times \left[\frac{G_{j,max} \times [\exp(A \times (V_j - V_{1/2}))] + G_{j,min}}{1 + [\exp(A \times (V_j - V_{1/2}))]}\right], \quad (3)$$

where $[PA]$ = the polyamine concentration added to the cell 1 patch pipette and $K_m(V_j)$ is the voltage-dependent dissociation constant for the polyamine from the Cx40 gap junction. The additional terms in Eq. 3 relative to Eq. 2 relate the amount of unblocked Cx40 gap junction channels to the G_j of the Cx40 gap junction. These results are consistent with a reversible concentration- and V_j-dependent blockade of Cx40 I_j by spermine.

Spermidine was a less potent blocker of Cx40 I_j than spermine as shown in Fig. 3 *B*. Ionic block was most pronounced at 15-mM spermidine, the maximal tolerable concentration, but far less effective than spermine at ten times the relative concentration. Spermidine has one less positively charged amino group ($z = +3$) and is shorter in length than spermine. The theoretical fits calculated using Eq. 3 and the experimentally derived $K_m(V_j)$ values for spermidine (see Table 1) are shown for the respective concentrations. These results are again consistent with reversible concentration- and V_j-dependent blockade of Cx40 I_j by spermidine.

TABLE 1 Dissociation constants for spermine and spermidine block of Cx40 I_j

Spermine		
V_j (mV)	K_m ± SE (mM)	
+4.3	25.349 ± 13.011	0.50
+8.6	4.943 ± 1.317	0.77
+13.2	1.618 ± 3.006	0.90
+18.0	0.670 ± 0.103	0.95
+23.1	0.351 ± 0.066	0.94
+27.9	0.233 ± 0.043	0.96
+32.8	0.151 ± 0.029	0.95
+37.7	0.107 ± 0.024	0.93
+42.8	0.076 ± 0.020	0.90
+47.8	0.076 ± 0.020	0.85
Spermidine		
V_j (mV)	K_m ± SE (mM)	
+4.5	186.88 ± 53.08	0.60
+8.8	61.55 ± 7.44	0.95
+13.3	25.92 ± 6.92	0.70
+17.8	26.22 ± 6.20	0.80
+22.4	15.74 ± 3.81	0.85
+27.3	10.66 ± 3.32	0.90
+32.4	7.20 ± 1.81	0.94
+37.6	5.34 ± 1.12	0.95
+42.7	4.73 ± 0.93	0.96
+47.9	5.36 ± 1.13	0.96

The mean g_j (± SD) was 3.01 ± 3.16 nS ($n = 3$) for 1 mM, 8.67 ± 5.08 nS ($n = 8$) for 2 mM, 2.82 ± 2.16 nS ($n = 5$) for 5 mM, 8.08 ± 4.34 nS ($n = 6$) for 10 mM, and 4.57 ± 2.52 nS ($n = 3$) for 15-mM spermidine. For all spermidine experiments, the average g_j was 5.42 ± 3.45 nS.

When 2-mM spermine was added unilaterally to cell 1 of a rat Cx43-transfected N2A cell pair, no reduction in I_j was observed. Fig. 4 compares the average steady state junctional I_j-V_j relationships from two normalized Cx43 experiments to the average data for Cx40 gap junctions in the presence of 2-mM spermine. The data presented for Cx40 is the same as shown in Fig. 3 *C*. In contrast to the decreasing I_j values for Cx40 at positive V_j values, the Cx43 I_j-V_j relationship at positive V_j was ohmic until V_j-gating commenced. The solid curve represents the observed V_j-dependence of Cx43 containing gap junctions according to Eq. 2 where $G_{j,min} =$ 0.32, $V_{1/2} = 60$ mV (−60 mV for negative V_j values), and $A = -0.10$ (+0.1 for negative V_j values) for a net gating charge of 2.5 elementary charges as described by Wang et al. (1992). The inability of spermine to block rCx43 I_j was also demonstrated in other laboratories (Shore et al., 2001).

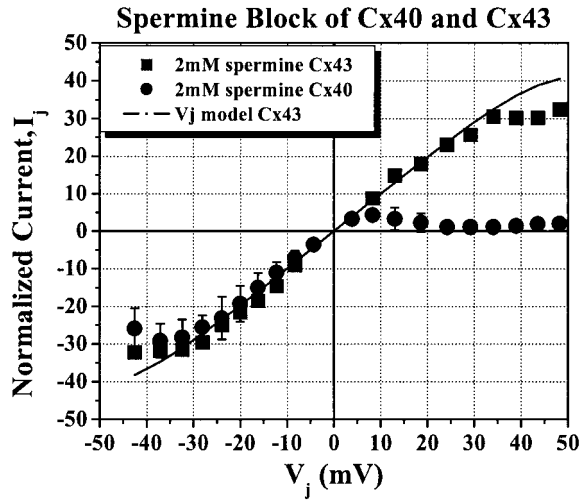

FIGURE 4 Comparison of the effects of 2-mM spermine on Cx40 and Cx43 gap junctions. Normalized steady-state junctional I_j-V_j relationships for both Cx40 and Cx43 gap junctions in the presence of 2-mM spermine added unilaterally to cell 1. The same junctional I–V curve shown in Fig. 3 for 2-mM spermine (●) is contrasted to the same for Cx43 (■), indicating that spermine did not significantly block Cx43 gap junctions. The solid line is the predicted junctional I–V relationship according to Eq. 2 using the V_j gating parameters for Cx43-containing gap junctions (Wang et al., 1992, see text for details).

Equilibrium constants for polyamine block

Voltage-dependent equilibrium constants

To determine the voltage-dependent equilibrium constants for polyamine block of rCx40 junctional currents, the fraction of unblocked steady-state current ($I_{(K+PA)}/I_{(K)}$) was plotted as a function of polyamine concentration for all experimental V_j values (Figs. 5, *A* and *B*). The dose response curves were then fitted with the following equation:

$$\frac{I_{j,K+PA}}{I_{j,K}} = \frac{1}{1 + ([PA]/K_m(V_j))}. \quad (4)$$

The $K_m(V_j)$ values obtained from the fits for both spermine and spermidine are provided in Table 1. These calculated equilibrium (dissociation) constants were used to model the steady state junctional I-V relationships for several concentrations of spermine and spermidine as shown in Figs. 3, *A* and *B*.

Estimation of the electrical distance to the site of polyamine block

The classic Woodhull (1973) model often used to describe the electrical distance (δ) to the site of voltage-dependent block by an impermeant or poorly permeable ion was rederived for a symmetrical (homotypic) gap junction channel (Musa et al., 2001). Because spermine appeared to block Cx40 gap junctions completely, only the expression for an impermeant blocker within a homotypic gap junction channel was used to fit the $K_m(V_j)$ values for spermine and spermidine. Fig. 6 shows the calculated fit of the experimental $K_m(V_j)$ values between +15 and +40 mV according to the equation:

$$K_m(V_j) = \left(\frac{b_{-1}}{b_1}\right) \times \exp\left(\frac{-zF\delta V_j}{RT}\right). \quad (5)$$

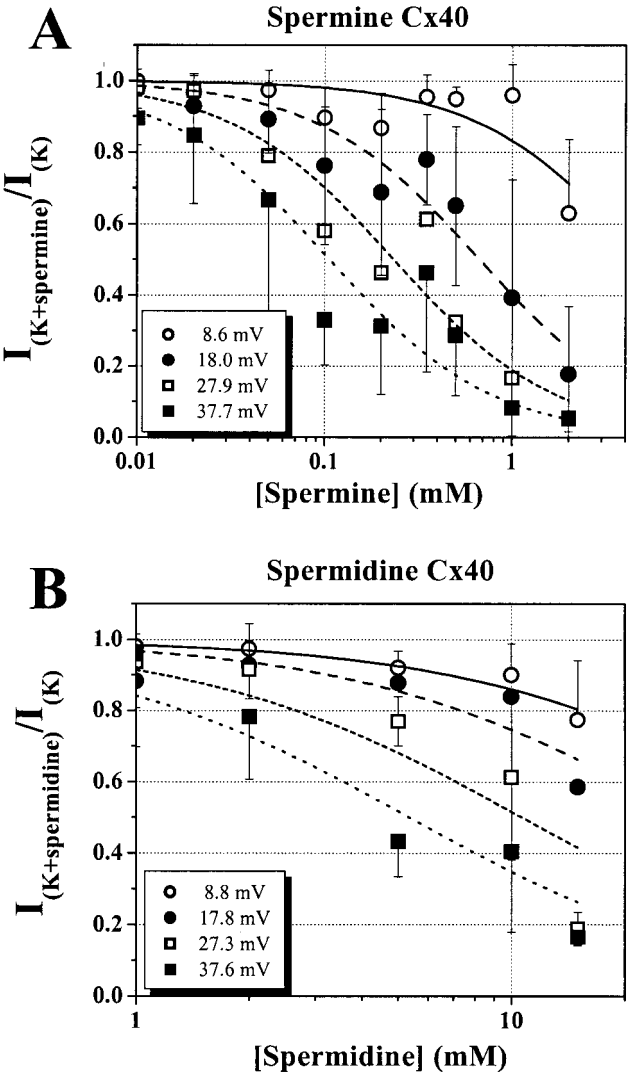

FIGURE 5 V_j-dependent dose-response curves for unilateral spermine and spermidine block of Cx40 I_j. The steady-state fraction of unblocked I_j was determined for each V_j value and concentration of spermine and spermidine. The steady-state I_j value at each positive V_j (block pulses) was divided by the steady-state I_j value at each corresponding negative V_j (control and recovery pulses averaged together) for each individual experiment. The steady-state fraction of unblocked I_j was plotted as a function of polyamine concentration for selected voltages and fit with Eq. 4 (see text for details). Each data point represents the mean ±SD for N experiments at each spermine and spermidine concentration. (*A*) Dose-response curves for spermine at the indicated V_j values. The curved lines are theoretical fits of the data and the parameters of the fits are listed in Table 1. (*B*) Dose-response curves for spermidine at the indicated V_j values. The curved lines are theoretical fits of the data and the parameters of the fits are listed in Table 1.

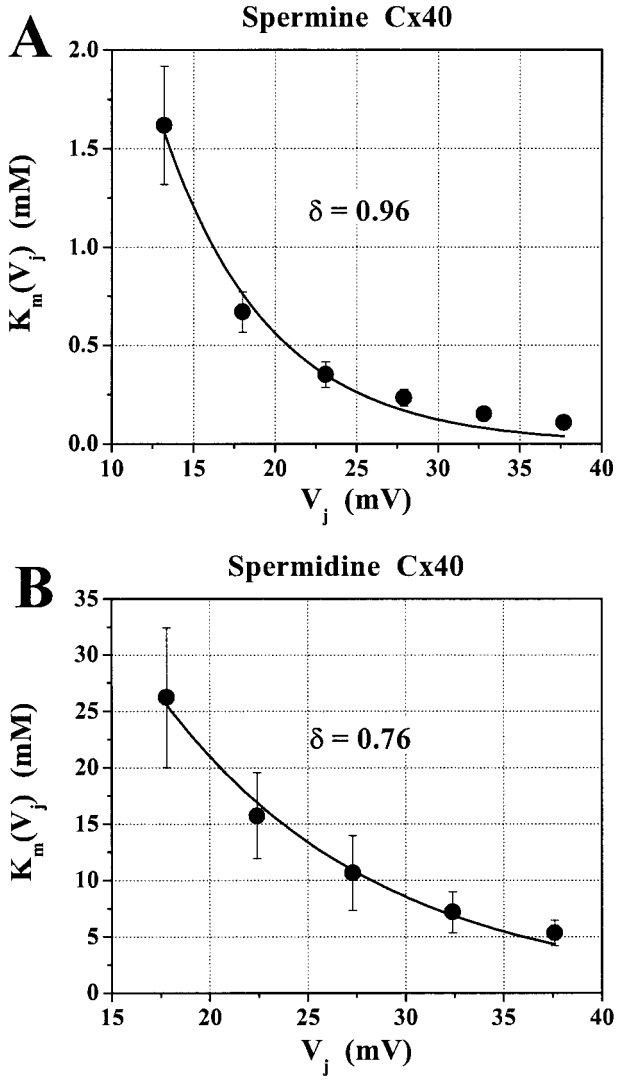

FIGURE 6 Theoretical fits of the V_j-dependent K_m values for spermine and spermidine. The K_m values within the experimental range of concentrations and $V_j \leq +40$ mV provided in Table 1 were fitted with Eq. 5 representing an analogous Woodhull (1973) model derivation for a homotypic gap junction blocked by an impermeant ion. The exact solutions to Eq. 5 are listed in Table 2. (*A*) The model predicts a δ value of 0.96 ± 0.07 for spermine, consistent with a single site of interaction that senses nearly 100% of the transjunctional voltage field. The equivalent valence of spermine used for the calculation was +4. (*B*) The model predicts a δ value of 0.76 ± 0.05 for spermidine with an equivalent valence of +3, consistent with a single site of interaction that senses ≅75% of the V_j field.

Only the $K_m(V_j)$ values in the linear portion of the junctional I-V relationships for each experiment were modeled to maintain the conditions of constant open probability. This condition necessitated the omission of all V_j values above ±40 mV where V_j-dependent gating commences, consistent with previous observations (Beblo et al., 1995; Veenstra, 2001). The estimated values of b_{-1}/b_1 and $z\delta$ for spermine and spermidine are listed in Table 2.

Given the valence of spermine ($z = +4$) and spermidine ($z = +3$) at physiological pH, the estimated values of δ from the mathematical fits of the $K_m(V_j)$ values were 0.96 ± 0.07 and 0.76 ± 0.05 for spermine and spermidine respectively. This implies that one spermine molecule can sense the entire transjunctional voltage field when associated with its corresponding site of block. By contrast, spermidine, can sense only ~75% of the V_j field across the rCx40 gap junction when associated with its corresponding site of block. The difference between the two polyamine δ values may reflect the proportion of I_j not blocked by spermidine under the existing experimental conditions, but this difference precisely equals the difference in valence between spermine and spermidine. Unfortunately, N2A cells were not able to tolerate intracellular concentrations of spermidine higher than 15 mM.

TABLE 2 $K_m(V_0)$ **and** $z\delta$ **values for block by spermine and spermidine**

Parameter	Spermine ($z = +4$)	Spermidine ($z = +3$)
b_{-1}/b_1 (y_0)	11.51 ± 0.75 mM	125.35 ± 16.95 mM
$z\delta$	3.84 ± 0.35	2.27 ± 0.16

Concentration-dependence of the voltage equilibrium constants

Fig. 6 examines the relationship between the equilibrium constants and transjunctional potential. To examine the effects of polyamine concentration on the voltage constant for equilibrium, the relative amount of unblocked junctional current was plotted as a function of spermine concentration. Fig. 7 illustrates the data for 10 μM, 50 μM, 100 μM, 1 mM, and 2 mM spermine fitted by the Boltzmann equation (Eq. 6). The results are listed in Table 3.

$$\frac{I_{(K+spermine)}}{I_{(K)}} = \left[\frac{I_{j,max} \times [\exp(A \times (V_j - V_{1/2}))] + I_{j,min}}{1 + [\exp(A \times (V_j - V_{1/2}))]}\right] \quad (6)$$

The value of I_{max} was fixed at 1.0 for all of the curves and the slope factor $A = zF/RT$. The $V_{1/2}$ and valence values for the 10-μM curve are equivalent to the Boltzmann parameters for the Cx40 G_j–V_j curve and are indicative of the onset of V_j gating at this minimum concentration of spermine (Veenstra, 2001). The decreasing Cx40 I_j with increasing concentrations of spermine is indicative of polyamine block. The $V_{1/2}$ occurs at the $K_m(V_j)$ for each spermine concentration and the $V_{1/2}$ for the 100 μM spermine concentration curve approximates the midpoint of the voltage axis, indicating that this concentration most closely approximates the equilibrium condition for this V_j protocol. The gating charge valence was ~3 for the 100-μM spermine concentration curve and did not exceed this value except for the three highest spermine concentrations tested experimentally. When the spermine concentration exceeded the $K_m(V_j)$ by a factor of two, the apparent gating charge doubles to six or more, indicating that more than one spermine molecule may bind at very high concentrations.

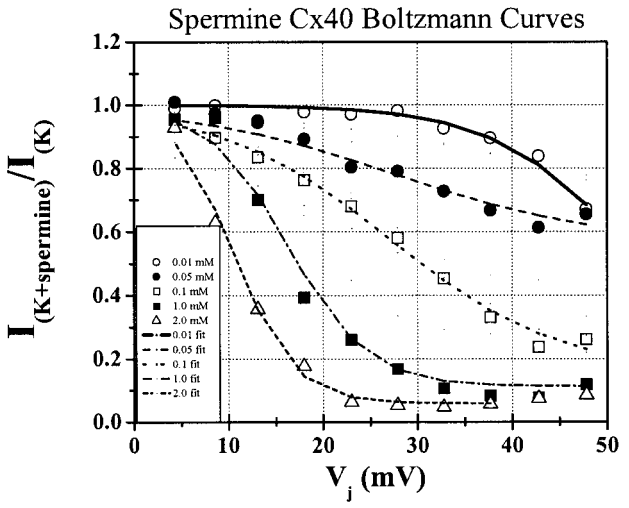

FIGURE 7 Voltage–Response curves for spermine block of Cx40 I_j. The steady-state fraction of unblocked I_j was plotted as a function of transjunctional voltage for all polyamine concentrations and fit with Eq. 6 (see text for details). Selected concentration curves are shown as symbols and the associated lines in the inset indicate the mathematical fits. The results for all spermine concentrations are provided in Table 3. The $V_{1/2}$ decreases and the slope increases with increasing spermine concentration.

Comparison of polyamine block to V_j gating of Cx40

The functional consequences of the kinetics of polyamine block are illustrated in Fig. 8 where three different voltage protocols were performed on the same preparation to compare the amount of block produced by 2-mM spermine. V_j was varied continuously from 0 to $\pm$100 mV with slopes of 200 or 600 ms/mV or in 10-mV increments with a pulse duration of 7.5 s and a 50% duty cycle. Previously, it was shown that a 200 ms/mV V_j ramp was sufficient to approximate the steady-state G_j-V_j relationship when compared to the conventional pulse protocol (Veenstra, 2001). This is evident for control $-V_j$ values in Fig. 8 *A* where the 200 ms/mV ramp, 600 ms/mV ramp, and pulse

TABLE 3 Boltzmann parameters of the Voltage–Response (V_j–I_j) curves

Concentration	I_{min}	$V_{1/2}$ (mV)	Valence (z)	Correlation coefficient
10 μM	0.08 ± 1.27	52.5 ± 16.3	3.5 ± 1.2	0.98
20 μM	0.59 ± 0.44	45.5 ± 30.8	1.7 ± 0.9	0.97
50 μM	0.56 ± 0.08	27.6 ± 5.3	2.3 ± 0.6	0.96
0.10 mM	0.15 ± 0.04	27.1 ± 1.2	2.8 ± 0.2	0.97
0.20 mM*	−0.11 ± 0.75*	33.3 ± 25.1	1.5 ± 0.9	0.83
0.35 mM	0.15 ± 0.19	32.5 ± 6.7	1.9 ± 0.4	0.94
0.50 mM	0.27 ± 0.01	18.3 ± 0.3	6.3 ± 0.4	0.97
1 mM	0.11 ± 0.02	16.3 ± 0.6	6.0 ± 0.7	0.92
2 mM	0.06 ± 0.01	10.6 ± 0.3	7.9 ± 0.7	0.94

*The V_{min} was not set to a fixed value and the data for 200-μM spermine produced a curve with a reduced slope and a poor fit as indicated by the correlation coefficient.

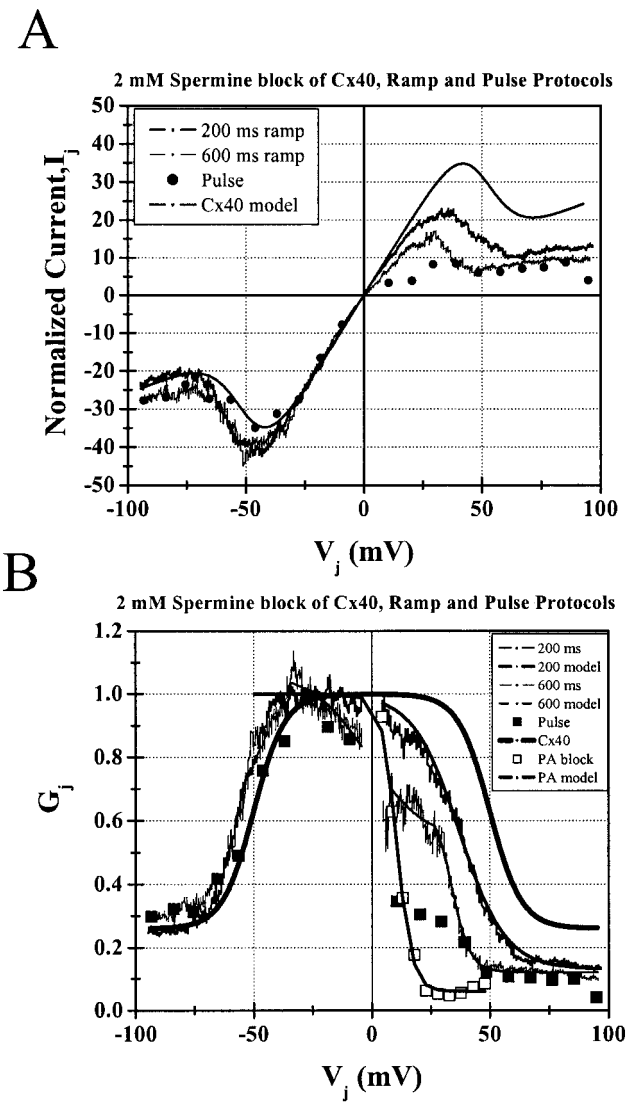

FIGURE 8 The effect of different voltage protocols on the block produced by unilateral 2-mM spermine. (*A*) Normalized steady-state junctional I–V relationships for Cx40 produced by continuous 200 ms/mV or 600 ms/mV voltage ramps and a 10-mV incremental pulse protocol over the same −100 to +100 mV V_j range. The pulse duration was 7.5 s with an equivalent duration recovery interval at ($V_j = 0$ mV). The normal V_j gating of Cx40 is modeled by the thick solid line. A progressive reduction in I_j is observed at positive V_j values with increasing ramp duration in the presence of 2-mM spermine in the whole cell patch pipette. The amount of block that developed during either V_j ramp did not attain the same level of block observed during the pulse protocol despite no difference in the V_j gating observed at negative V_j values. (*B*) The same data as in panel A except the I_j values were converted to G_j values by dividing by V_j. The 200 and 600 ms/mV G_j-V_j curves were fit with Boltzmann equations (Eq. 7) and the parameters of the model curves are provided in Table 3. The pulse protocol data was not fitted to a Boltzmann function, but the Boltzmann curve for 2-mM spermine as shown in Fig. 7 is provided for comparison. It is apparent that the 7.5-s duration pulses did not achieve the full amount of block observed with the 30-s duration pulses (see Figs. 1 and 2).

protocol steady-state junctional I-V curves agree closely with the model derived from the results of Veenstra (2001). However, much less block is evident at $+V_j$ values with the 200 ms/mV ramp compared to the pulse protocol. A 600 ms/mV ramp was performed on the same preparations and produced an intermediate amount of block that eventually achieved the maximum amount of block at voltages $\geq +50$ mV. Each I-V curve represents the average of three experiments on which all three V_j protocols were completed. The average g_j was 2.86 ± 1.52 nS for the 200 ms/mV ramps, 2.03 ± 0.83 nS for the 600 ms/mV ramps, and 1.65 ± 0.41 nS for the pulse protocol.

The junctional G-V curves are shown in Fig. 8 *B* and display a characteristic morphology of heterotypic connexin gap junctions (Verselis et al, 1994; Valiunas et al., 2000). The 200 ms/mV data was fit with a single Boltzmann distribution (Eq. 7) whereas the 600 ms/mV ramp required the sum of two Boltzmann functions to describe the shape of the curve.

$$\mathsf{G_j} = \left[\frac{\mathsf{G_{j,max}} \times [\exp(\mathsf{A} \times (\mathsf{V_j} - \mathsf{V_{1/2}}))] + \mathsf{G_{j,min}}}{1 + [\exp(\mathsf{A} \times (\mathsf{V_j} - \mathsf{V_{1/2}}))]}\right] \quad (7)$$

The parameters of the fits are provided in Table 4. The G_{max} was not fixed for these procedures to obtain an estimate of the amount of block at 0 mV. The higher than unity G_{max} for the more heterotypic appearing 600 ms/mV ramp indicates that there was block at 0 mV of ~7%. G_{max} was 4% reduced from control Cx40 values during the 200 mS/mV ramp. The $K_m(V_0)$ is estimated to be 11.5 mM according to the solution to Eq. 5 and predicts 8% occupancy of the Cx40 channels with 2-mM spermine. The final value of G_{min} was the same for both ramps at 0.12 compared to the expected value of 0.06 for 2-mM spermine from Table 3. The gating charge valence was 2.6 for the faster V_j ramp, in close agreement with the fits of the lower spermine concentrations listed in Table 3. The 600-ms ramp exhibits two Boltzmann distributions, one centered around 0 ± 30 mV with a slope corresponding to a gating charge valence of 2.1 and a second component with a slope of 6.4 and a $V_{1/2}$ of 34 mV. The slope of the second Boltzmann is consistent with the values observed for the high spermine concentrations in Table 3, suggesting that more than one spermine molecule may be associating with the Cx40 channel during the longer duration ramp. The data from the shorter duration pulse protocol was not at the steady-state values determined from similar V_j pulses of four times the duration (7.5 versus 30 s). This suggests that there are two components to the complete block by spermine. The first component develops with time constants in the 100-ms range while the second component takes seconds to develop.

Bilateral block of Cx40 gap junctions by spermine

The observation that unilateral spermine produced asymmetric junctional I-V curves led us to apply spermine bilaterally. The results of these experiments are shown in Fig. 9. Only the block protocol described in Fig. 2 was used to examine the extent of bilateral block by high doses of spermine. The resulting junctional I-V and G-V curves were symmetric, demonstrating that spermine blocks equally well from both sides despite any evidence that it can permeate the Cx40 gap junction. The magnitude of the block appears to be reduced compared to the results with unilateral spermine (Fig. 9 *A*), but this is attributed to the presence of a finite amount of block at 0 mV as observed in Fig. 8. The bilateral spermine G_j-V_j curves were fit with Eq. 7 as indicated by the solid line in Fig. 9 *B* and the results are presented in Table 5. The reduced G_j values are indicative of block by spermine at 0 mV that increases in both directions. The maximum block by bilateral 2-mM spermine occurred with a $V_{1/2}$ of ~17.2 ± 0.4 mV, assuming a $G_{j,max}$ of 0.92 and G_{min} of 0.07. The data are consistent with a single spermine molecule blocking from each side with identical $K_m(V_j)$ values. The average g_j for the three 2 mM bilateral spermine experiments was 1.82 ± 1.20 nS.

Kinetics of spermine block of rCx40 I_j

Spermine did not block any portion of Cx40 I_j instantaneously. The time dependence of spermine block was determined by fitting the decay phase of I_j at $+V_j$ with a single exponential function. Fig. 10 *A* plots the decay time constant (τ) as a function of V_j for 100 μM (◆), 350 μM (▼), 500 μM (●), 1 mM (▲), and 2 mM (■) spermine. All fitted time constants ranged from 70 to 6000 ms and exhibited significant voltage and concentration dependence. While these time constants appear slow relative to the time dependence for ionic block of other membrane channels ($\tau < 10$ ms), it is consistent with gap junction channel kinetics being ~1000-fold slower than those observed for most ion channels. The on rates (k_1) were determined from the time constants utilizing the equation:

$$\mathsf{k_1} = \frac{1}{\tau \times [\mathsf{PA}]}. \quad (8)$$

TABLE 4 Boltzmann parameters of the nonsteady-state G_j–V_j curves

Protocol	G_{max}	G_{min}	$V_{1/2}$ (mV)	Valence (z)	Correlation coefficient
200 ms/mV	0.96 ± 0.004	0.13 ± 0.02	37.1 ± 0.1	2.6 ± 0.04	0.95
600 ms/mV	1.07 ± 0.01	0.54 ± 0.02	−1.4 ± 0.8	2.1 ± 0.2	0.96
600 ms/mV	0.66 ± 0.01	0.12 ± 0.001	33.9 ± 0.2	6.4 ± 0.2	0.93

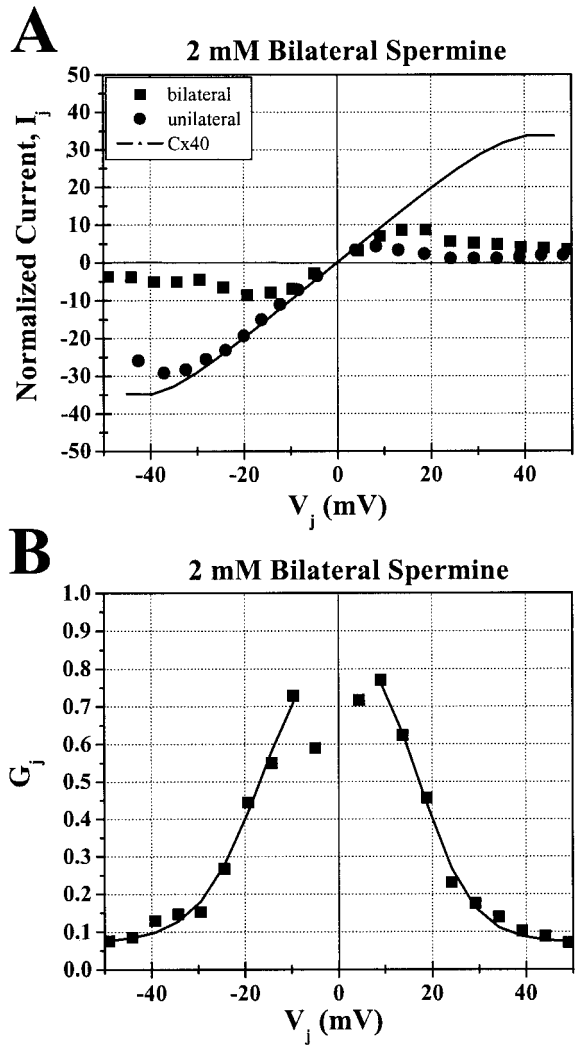

FIGURE 9 Bilateral addition of 2-mM spermine. (*A*) The normalized steady-state junctional I–V curves for the unilateral (●) and bilateral (■) addition of 2-mM spermine. The solid line indicates the V_j gating of Cx40 g_j. Less I_j block is apparent under bilateral conditions. (*B*) The normalized steady state G_j-V_j curve for the bilateral spermine data shown in panel A is plotted and fitted with Eq. 7 (*solid lines*). The Boltzmann parameters are given in Table 5. The results are consistent with one spermine molecule binding equally well from either side with a $V_{1/2}$ of ~17 mV.

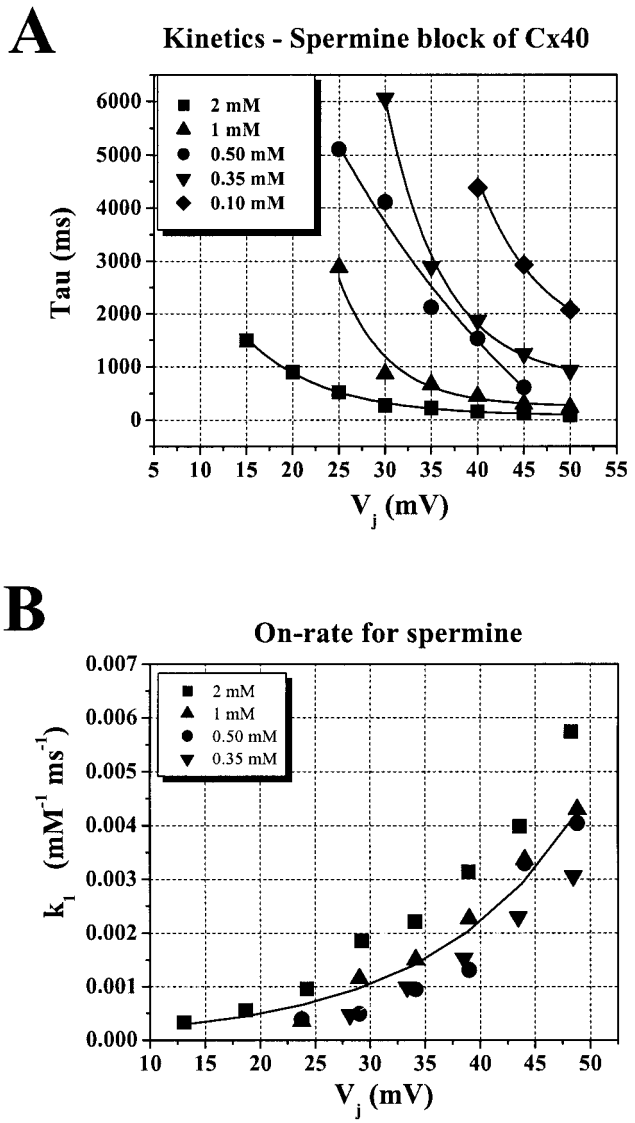

FIGURE 10 Kinetics of I_j block at various spermine concentrations. (*A*) The decay of I_j was described by a single exponential function and the time constants (τ) were plotted as a function of V_j for each spermine concentration. Only the decay phase of I_j at positive V_j values in the presence of 100 μM (◆), 350 μM (▼), 500 μM (●), 1 mM (▲), and 2 mM (■) spermine were analyzed. Estimated values of τ were within the range of 70–6000 ms. (*B*) On-rate constants (k_1) plotted as a function of V_j. The values for k_1 were calculated from the values of τ shown in panel A according to Eq. 8 (see text for details). A single exponential fit of all of the k_1 values except 100 μM is represented by the solid line and predicts an e-fold change in the on-rate constant for every 13.55 mV (see Eq. 9).

In Fig. 10 *B*, the calculated k_1 values for the data presented in the previous figure were plotted as a function of V_j for 350 μM, 500 μM, 1 mM, and 2 mM spermine. The 100-μM data were not used because there were only three points, the minimum number required to define a nonlinear function.

TABLE 5 Boltzmann parameters of the G_j–V_j curves with bilateral 2-mM spermine

Protocol	G_{max}*	G_{min}*	$V_{1/2}$ (mV)	Valence (z)	Correlation coefficient
$-V_j$	0.92	0.07	−16.9 ± 0.4	−3.83 ± 0.23	0.94
$+V_j$	0.92	0.07	+17.5 ± 0.3	4.48 ± 0.23	0.95

*The G_{max} and G_{min} values were fixed to avoid negative G_{min} values.

The pooled data were fit with a single exponential function (*solid line*, Fig. 10 *B*):

$$k = y_0 \times \exp\left(\frac{V_j}{V_k}\right), \quad (9)$$

where y_0 is the amplitude at 0 mV and V_k is the voltage constant that predicted an e-fold change in the on rate for every 13.55 mV (Table 6).

TABLE 6 On and off rates for spermine block of Cx40 I_j

Rate	Amplitude (y_0)	Voltage constant (V_k)
On rate (k_1) (from τ)	0.00033 ± 0.009 ms^{-1} mM^{-1}	13.5 ± 1.7 mV
On rate (k_1) (from Eq. 9)	0.00045 ± 0.0009 ms^{-1} mM^{-1}	13.5 ± 0.0 mV
Off rate (k_{-1})* (from Eq. 9)	0.026816 ± 0.012745 ms^{-1}	4.2 ± 0.1 mV

*k_{-1} asymptotes to 0.000773 ± 0.000404 at large positive V_j values.

Attempts to fit the recovery phase of I_j (see Fig. 1) to determine the off-rate constants (k_{-1}) were unsuccessful due to varying magnitudes of time-independent and slow time-dependent unblock kinetics. Instead the off rates were calculated using the following equation:

$$K_m = \frac{k_{-1}}{k_1}. \quad (10)$$

The K_m values refer to our experimentally derived equilibrium constants (see Table 1) and the k_1 values were calculated using the exact solution provided by the single exponential fit of the calculated k_1 values at the each $K_m(V_j)$ (*solid line*, Fig. 11 *B*). The solutions to Eq. 9 for the on and off rates are also provided in Table 6. The results for k_{-1} are plotted in Fig. 11 *A*. Fig. 11 *B* combines data from Figs. 10 *B* and 11 *A*, plotting both rate constants as a function of V_j. As expected from bimolecular kinetics, k_{-1} is more voltage-sensitive than k_1. The predicted $V_{1/2}$ for the bimolecular interaction was 15.6 ± 1.0 mV.

We were able to estimate the recovery time constant from four 2-mM spermine experiments during the initial 50-ms segment immediately after polarity reversal from a $+V_j$ to a $-V_j$ step of equal amplitude (recovery). An appreciable amount of unblock (30–40% of the total recovery from block) occurred during this time interval. Exponential fits of this rapid portion of unblock produced time constants ranging from 10 to 20 ms. For comparison, we estimated the value of τ for unblock using Eq. 9. The K_m value for −40 mV of 5.192 M was calculated from the solution to Eq. 5 (see Fig. 5 *A*, *solid line*): $K_m = 11.51 \times \exp[-(3.8442 \times V_j)/25.42]$. The calculated value for k_1 at −40 mV according to Eq. 9 was 2.37×10^{-5} (mM^{-1} ms^{-1}). Combining these estimates in Eq. 10 predicted a $1/k_{-1}$ value of 8 ms at $V_j = -40$ mV in the presence of 2-mM spermine. This estimate was in close agreement with our experimental observations. The temporal resolution of our experimental data was also limited by the low pass bandwidth of 100 Hz used to acquire 90 continuous seconds of whole cell currents per V_j value. The response time for a full amplitude event under these conditions was 6.4 ms.

Single channel analysis of spermine block of the rCx40 channel

All data presented in the previous figures were obtained from macroscopic recordings of rCx40 I_j. Occasional lower conductance recordings were encountered ($g_j < 1$ nS) that permitted the examination of unitary channel conductance (γ_j) and open probability (P_o). The voltage protocol was modified to include only the 20–40 mV V_j range and the step duration was increased from 30 to 60 seconds. One example of a multichannel recording in the presence of 2-mM spermine is shown in Fig. 12. The junctional whole cell currents in panels (*A* and *E*) show multichannel activity at negative V_j values relative to cell 1. The corresponding all points histograms, shown in panels (*B* and *F*), in which peaks representative of three, four, five, and six open channels predominate. When V_j is positive relative to cell 1, the whole cell junctional currents (*panel C*) show a dramatic

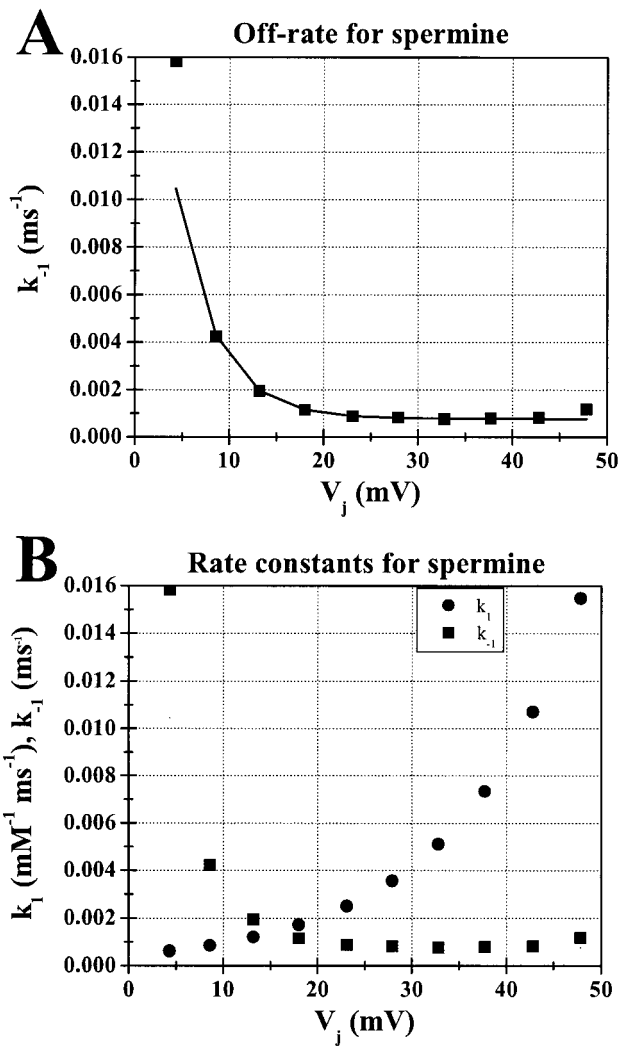

FIGURE 11 V_j-dependent off-rate constants (k_{-1}) for spermine. (*A*) Values for k_{-1} were calculated utilizing Eq. 10 from the derived values for k_1 (Fig. 10 *B*) and the voltage-dependent K_m values (Table 1). The data points (■) were fit with a single exponential function that predicts an e-fold change in the off rate for every 4.2 mV, threefold more sensitive to V_j than the corresponding k_1 function (Eq. 8). (*B*) Comparison of the k_1 and k_{-1} rate constants at the same V_j values. The k_{-1} data points are the same as those presented in panel A and the calculated k_1 values (●) for each corresponding V_j as shown in Fig. 10 *B*.

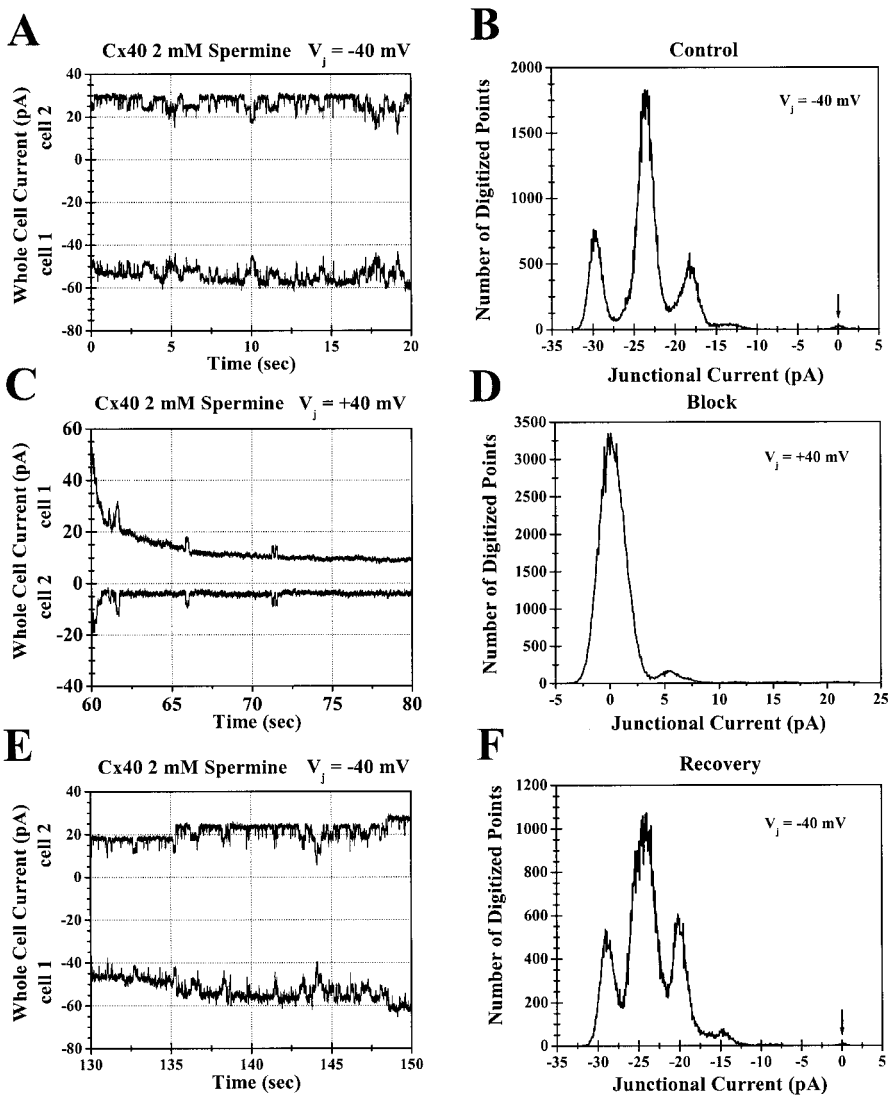

FIGURE 12 Blockade of Cx40 unitary channel currents by 2-mM spermine. Panels A–F are representative of a −/+/− 40 mV V_j sequence obtained from a Cx40 cell pair with low g_j (<1 nS). Panels A, C, and E illustrate a 20-s excerpt displaying all of the multiple channel levels observed during each V_j pulse with IPS KCl in both pipettes and 2-mM spermine added unilaterally to cell 1. Each V_j pulse was 60 s in duration for this experiment. Panels B, D, and F are the all points junctional current amplitude histograms for each entire 60-s V_j step. Up to six unitary channels are observed in control (*A* and *B*) and recovery (*E* and *F*) −40 mV V_j pulses with the predominant peaks representing four, five, and six open channels. During the +40 mV blocking pulse (*C* and *D*), only a small peak representing one open channel is evident in the histogram indicating that spermine blocked all six channels for the majority of the 60-s voltage step.

reduction in channel activity within the first five seconds of the voltage step followed by very infrequent single channel openings for the remainder of the V_j step. The data demonstrate a reversible reduction in P_o when V_j is positive with respect to the spermine-containing cell. This is confirmed by the accompanying all points histogram displaying a single observable peak representing the opening of only one channel at a time. Peak-to-peak current amplitudes from all of the real time histograms were plotted as a function of transjunctional voltage and fit by linear regression (Fig. 13). The unitary junctional I-V relationship had a linear slope conductance of 129 ± 6.4 pS. This γ_j value in the presence of 2-mM spermine was slightly lower (14 ± 3.5%) than expected for the 150-pS main conductance state of the rat Cx40 channel (Musa et al., 2001).

DISCUSSION

The tetraalkylammonium series of monovalent cations and the polyamines are two forms of ions that block several types of ion channels, including gap junctions (French and Shoukimas, 1985; Yellen, 1987; Scott et al., 1993; Williams, 1997; Musa et al., 2001). Regarding gap junction channels, the polyamines have two relevant advantages over the larger tetraalkylammonium ions. Spermine and spermidine are endogenous to cardiomyocytes, and all eukaryotic cells, and spermine completely blocks Cx40 gap junctions (Fig. 1–3). TPeA and THxA ions must be introduced into cells and only partially inhibit Cx40 g_j. TPeA also inhibits Cx43 g_j in a similar manner to Cx40 and likely is a nonspecific blocker of most connexin-specific gap junctions (Veenstra, 2000). Spermine appears to act specifically on Cx40 and not Cx43, thus providing a selective mechanism for blocking Cx40-containing gap junctions (Fig. 4). It remains to be determined if spermine will similarly inhibit heteromeric gap junctions containing Cx40.

A primary goal in determining the voltage-dependent block of homotypic gap junction channels by organic cations is to identify a specific site for block within the permeation

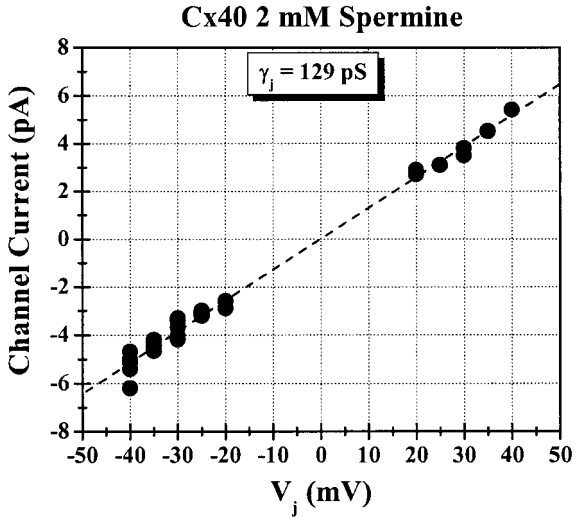

FIGURE 13 Single channel junctional I–V relationship in the presence of 2-mM spermine. The unitary current amplitudes of the Cx40 channels present in the experiment shown in Fig. 9 (*panels B*, *D*, and *F*) were plotted as function of V_j and a linear regression fit was performed on all data points. The fit yielded a mean single channel slope conductance (γ_j) of 129 pS for the open Cx40 channels in the presence of 2-mM spermine.

pathway of a gap junction channel. Spermine and spermidine both provided physically realistic estimates of the electrical distance for block within the Cx40 channel that coincides with the number of positively charged amino groups on the blocking molecule. This suggests that the complete closure of the Cx40 gap junction channel by a voltage-dependent mechanism required a net valence of +4. This was also described by Veenstra (2001) when examining the endogenous V_j-gating of Cx40 g_j. The δ value of 0.96 for spermine ($z = +4$) indicates that this molecule senses the entire V_j field while it occludes the Cx40 pore whereas the δ value for spermidine ($z = +3$) was only 0.76 (Fig. 6). The present data do not identify the exact location of the polyamine-binding site on the Cx40 protein.

Given that the homotypic Cx40 gap junction is a symmetrical channel, Eq. 5 is valid only if spermine blocks from both sides. Figs. 8 and 9 demonstrate that the unilateral addition of spermine produces a heterotypic phenotype while the presence of spermine bilaterally results in a symmetrical G_j-V_j curve. The $V_{1/2}$ values for spermine block were all reduced relative to the endogenous V_j gating of Cx40 and can be interpreted as an enhancement of the endogenous V_j gating of Cx40 or as a distinct blocking mechanism with a lower $V_{1/2}$. Fig. 8 clearly demonstrates that the block by unilateral spermine develops more slowly and reduces G_j to a lower G_{min} value than is present during the endogenous V_j gating of Cx40. Spermine is positively charged which means it has the same polarity as the proposed V_j gate for Cx40 (Valiunas et al., 2000). Spermine also possesses bilateral symmetry and is not likely to serve as an intermediate between two intramolecular domains of opposite charge. When spermine is present in high concentration ($>K_m(V_j)$) on both sides of the gap junction, it blocks equally well from either side with a $V_{1/2}$ that is in close agreement with the $V_{1/2}$ for the first order kinetic rate constants for the interaction of spermine with Cx40. The on and off rates for spermine are voltage-dependent, with k_{-1} being approximately threefold more sensitive than k_1 (Figs. 10 and 11). This is consistent with conventional first-order bimolecular kinetic reaction rates where k_1 is also concentration dependent and the equilibrium (dissociation) constant ($K_m(V_j)$) is determined by the ratio of k_{-1}/k_1 (Eqs. 8–10, Figs. 6, 10, and 11) (Anderson et al., 1988). The kinetics of block and unblock for spermine's interaction with Cx40 are on the order of 100 ms^{-1} and the $K_m(V_j)$ values are on the order of 100 μM (Fig. 5 and Table 1). The experimentally derived reaction rates and equilibrium constants at positive voltages also fairly accurately predict rapid dissociation rates and molar $K_m(V_j)$ values at negative V_j values. These values are at least an order of magnitude higher than the observed interaction of spermine with the IRK1 channel ($K_m(V_j) = 10$ μM; Ficker et al., 1994; Lopatin et al., 1994).

Charged amino acid residues located near the amino terminus have been implicated in determining the polarity of closure for Cx26 and Cx32 (Verselis et al., 1994; Oh et al., 2000). It was originally proposed that each gap junction hemichannel possesses its own V_j gate that closes when V_j is of like polarity, thus sensing the entire voltage drop across the junction (Harris et al., 1981; Spray et al., 1981). The ''ball and chain'' model for N-type inactivation in some forms of voltage-gated potassium channels proposed that an inactivation ball, made up of a concentration of positive residues near the amino terminus of the potassium channel protein, occludes the pore when appropriate by a bimolecular interaction (Hoshi et al., 1990). These positively charged residues associate with negative residues (receptor) found within or near the pore of the cation selective ion channel (Isacoff et al., 1991). Inactivation (block) of the ion channel results when a mobile part of the protein (ball) occludes the pore of the open channel and blocked the flow of permeable ions. Experiments examining the block of potassium channels by another quaternary ammonium compound, triethylnonylammonium, an ion with a positively charged headgroup and a long hydrophobic tail also support a form of the ball and chain mechanism of ion channel block (Armstrong, 1971).

It is possible that polyamines act in association with a specific intracellular domain of the Cx40 protein by a mechanism similar to the ''ball and chain'' N-type inactivation. It is possible that spermine and, to a lesser extent, spermidine serve as an exogenous gating particle to the endogenous V_j-receptor of Cx40. We subsequently tested several diaminoalkane compounds, including the divalent polyamine putrescine (1,4-diaminobutane), and found that none of the diaminoalkanes from 1,3-diaminopropane to 1,10-diaminodecane produced any significant block of Cx40

g_j within the ±50 mV V_j range (data not shown). The lack of block by 1,10-diaminodecane is in contrast to the results with those forms of *N*-methyl-D-aspartate (NMDA) receptors and the inward rectifier IRK1 that are blocked by spermine and related polyamines (Rock and Macdonald, 1992; Ficker et al., 1994; Lopatin et al., 1994). The observation that spermine block takes longer to develop than the endogenous V_j gating of Cx40 could result from the requirement that spermine must first associate with open Cx40 channels from bulk solution.

The hypothesis that the polyamines act as an inactivation particle is further supported by the evidence that the reduction in g_j is due primarily to a reduction in channel P_o rather than γ_j (Fig. 12 and 13). Time-dependent block resulting in reductions in P_o is indicative of a slow block resembling channel gating rather than flickery open channel block by an ion permeation mechanism which typically produces apparent channel subconductance states (Hurst et al., 1995). Voltage-dependent flickery block resulting in reductions in single channel conductance were observed with spermine and other polyamines on the NMDA receptor (Rock and Macdonald, 1992). In the inward-rectifying K^+ channels, the site of block is a single aspartate (D172) residue that resides deep within the pore common to the rapid flickery block induced by Cs^+ and Rb^+ (Ficker et al., 1994; Wible et al., 1994; Abrams et al, 1996). There was also a time-dependent kinetic component to the polyvalent cation block of IRK1 that was attributed to a second blocked state of the strong inward rectifier K^+ channel (Lopatin et al., 1995; Yang et al., 1995; Lee et al., 1999; Guo and Lu, 2000b). This slow time-dependent blocked state involves interactions with a glutamate residue (E224) on the cytoplasmic carboxyl tail domain to form an intrinsic gating complex that also occludes the IRK1 pore (Lee et al., 1999). Intracellular spermine similarly produced multiple blocked states of the retinal cGMP-gated channel that is affected by an E363G mutation involved in divalent cation block and determination of the single channel conductance (Lu and Ding, 1999; Gou and Lu, 2000a). The differing duration V_j protocols presented in Fig. 8 also suggest that there is a lesser magnitude ultraslow ($\tau \geq s$) component to the spermine block of Cx40 g_j. However, this difference in spermine block of the Cx40 channel occurred with varying duration voltage protocols where the intrinsic V_j gating of Cx40 was unaltered by these same voltage clamp procedures.

The observed polyamine block of Cx40 resembles the block of the fast vacuolar (FV) channel where it was observed that either one spermine or two putrescine molecules (net $z = +4$) were required to block the channel (Dobrovinskaya et al., 1999). Spermidine, with an intermediate valence of +3, required almost a 10-fold increase in the $K_m(V_j)$ to produce the same effect as spermine. The $K_m(V_j)$ for putrescine was 50-fold higher than spermine in the FV channel. The FV channel polyamine block also produced an 80% reduction in the cumulative open channel current with less than a 20% reduction in the single channel current amplitude. In our experiments, putrescine was not well tolerated by cells at concentrations ≥30 mM and failed to produce any block of the Cx40 channel (data not shown). A small diminution in γ_j of ~15%, from 150 to 129 pS, was also observed for the Cx40 channel in the presence of 2-mM spermine. A decrease in γ_j can be due to screening of negative charge associated with a channel pore (Dani, 1986; Green et al., 1987; Imoto et al., 1988; Green and Andersen, 1991). However, no apparent shift in the V_j gating of Cx40 g_j occurred, as expected from the screening of critical charged residues. Furthermore, charge alterations in the IRK1 channel that antagonize the polyamine block did not alter channel conductance (D172N mutant IRK1 channel, Ficker et al., 1994). Additionally, mutations (L385N) to the receptor for the N-terminal inactivation ball that did not alter protein charge did reduce channel conductance slightly in the *Shaker* K^+ channel (Isacoff et al., 1991). There were indications that 2-mM spermine associates with the Cx40 protein even at 0 mV and this 8% reduction in G_{max} may result from the slight reduction in γ_j (Figs. 8 and 13).

The possible physiological relevance of the spermine block on Cx40 g_j is substantiated by the observation that the $K_m(V_j)$ values are within the expected levels of free intracellular spermine concentrations. Essentially all of the $K_m(V_j)$ values for $V_j \geq +20$ mV are in the 100-μM range that are known to increase rectification of the IK1 currents in rat ventricular cardiomyocytes (Lopatin et al., 2000). This suggests that endogenous spermine can produce significant block of Cx40 gap junctions whenever a steady-state V_j gradient of >20 mV exists between neighboring cells for 5 s or less. Because free polyamine levels can be increased by lowering ATP levels or increasing ornithine decarboxylase activity, spermine block of Cx40 gap junctions could have a more prominent role in cardiac hypertrophy, myocardial ischemia, and β-adrenergic stimulation induced arrhythmias (Nichols et al., 1996; Bergeron et al., 1998). Natural spermine analogs are found in certain spider and wasp venoms and likely exert their toxic effects on neuronal NMDA and nicotinic acetylcholine receptor channels in addition to the inward rectifier K^+ channels (Donevan and Ragowski, 1996; Nichols et al., 1996; Haghighi and Cooper, 1998; Ruppersberg, 2000). These polyamine-related toxins typically have a large hydrophobic headgroup that prevents them from traversing the cell membrane or the channel pore and thus act extracellularly. The possible relevance of Cx40 blockade by spermine to cardiac action potential propagation is presently being investigated.

In conclusion, the experimental data demonstrates that spermine blocks Cx40 gap junctions in a voltage- and concentration-dependent manner. This block is specific to Cx40 because equal concentrations of spermine did not affect Cx43 g_j. The voltage-dependent equilibrium constants are within the physiological range of intracellular spermine concentrations with transjunctional voltage differences of

only 20 mV or more. The kinetics of unilateral block was on the order of hundreds of milliseconds to seconds and was rapidly reversible upon transposition of the intercellular voltage gradient. The reduction in g_j is predominantly produced by a dramatic increase in the closed time of the Cx40 channel, consistent with a kinetically slower form of block that resembles channel gating between open and closed states rather than rapid ionic block of the open channel that results in flickering. It is proposed that spermine, and minimally spermidine, act as physiological modulators of Cx40 gap junctions. The action of the polyamines is consistent with a reversible, first-order, voltage-dependent association with the ionic permeation pathway of Cx40 gap junctions. This association results in occlusion of the channel in a manner analogous to the endogenous V_j gating of Cx40. These are the first observations of an ionic mechanism for complete blockade of a gap junction channel that is also connexin-specific. These observations may lead to the identification of specific amino acid residues that form key elements of the channel opening and V_j gate of the Cx40 protein.

We want to thank Sophia Tashkovski, Stephanie DiPerna, Lynette Santana, Nan Pan, Michelle Kuhfta, and Erica Deibert for their technical assistance in the preparation and maintenance of the Cx40-transfected N2A cells. Dr. Eric C. Beyer graciously provided the rat Cx40 cDNA. This work was supported by National Institutes of Health (grant R01 HL-42220 to RDV and grant HL-45466 to RDV and ECB).

REFERENCES

Abrams, C. J., N. W. Davies, P. A. Shelton, and P. R. Stanfield. 1996. The role of a single aspartate residue in ionic selectivity and block of a murine inward rectifier K^+ channel Kir2.1. *J. Physiol. (Lond.)*. 493:643–649.

Anderson, C. S., R. MacKinnon, C. Smith, and C. Miller. 1988. Charybdotoxin block of single Ca^{2+} -activated K^+ channels. Effects of channel gating, voltage, and ionic strength. *J. Gen. Physiol*. 91:317–333.

Armstrong, C. M. 1971. Interaction of tetraethylammonium ion derivatives with the potassium channels of giant axons. *J. Gen. Physiol*. 58:413–437.

Beblo, D. A., and R. D. Veenstra. 1997. Monovalent cation permeation through the connexin40 gap junction channel. Cs, Rb, K, Na, Li, TEA, TMA, TBA, and effects of anions Br, Cl, F, acetate, aspartate, glutamate, and NO_3. *J. Gen. Physiol*. 109:509–522.

Beblo, D. A., H.-Z. Wang, E. C. Beyer, E. M. Westphale, and R. D. Veenstra. 1995. Unique conductance, gating, and selective permeability properties of gap junction channels formed by connexin40. *Circ. Res.* 77:813–822.

Bergeron, R. J., J. Wiegand, W. R. Weimar, and P. S. Snyder. 1998. Polyamine analogue antiarrythmics. *Pharm. Res*. 38:367–380.

Beyer, E. C., D. L. Paul, and D. A. Goodenough. 1990. Connexin family of gap junction proteins. *J. Membr. Biol*. 116:187–194.

Beyer, E. C., and K. Willecke. 2000. Gap junction genes and their regulation. *In* Gap Junctions, Advances in Molecular and Cell Biology, Vol. 30. E. L. Hertzberg, editor. JAI Press, Stamford. 1–30.

Dani, J. A. 1986. Ion-channel entrances influence permeation. *Biophys. J*. 49:607–618.

Dobrovinskaya, O. R., J. Muñiz, and I. I. Pottosin. 1999. Inhibition of vacuolar ion channels by polyamines. *J. Membrane Biol*. 167:127–140.

Donevan, S. D., and M. A. Ragowski. 1996. Multiple actions of arylalkylmine arthropod toxins on the N-methyl-D-asparate receptor. *Neuroscience*. 70:361–375.

Elfgang, C., R. Eckert, H. Lichtenberg-Frate, A. Butterweck, O. Traub, R. A. Klein, D. Hülser, and K. Willecke. 1995. Specific permeability and selective formation of gap junction channels in connexin-transfected HeLa cells. *J. Cell Biol*. 129:805–817.

French, R. J., and J. J. Shoukimas. 1985. An ion's view of the potassium channel. The structure of the permeation pathway as sensed by a variety of blocking ions. *J. Gen. Physiol*. 85:669–698.

Ficker, E., M. Taglialatela, B. A. Wible, C. M. Henley, and A. M. Brown. 1994. Spermine and spermidine as gating molecules for inward rectifier K+ channels. *Science*. 266:1068–1072.

Green, W. N., and O. S. Anderson. 1991. Surface charge and ion channel function. *Annu. Rev. Physiol*. 53:341–359.

Green, W. N., L. B. Weiss, and O. S. Anderson. 1987. Batrachotoxin-modified sodium channels in planar lipid bilayers. Ion permeation and block. *J. Gen. Physiol*. 89:841–872.

Goodenough, D. A., J. A. Goliger, and D. L. Paul. 1996. Connexins, connexons and intracellular communication. *Annu. Rev. Biochem*. 65:475–502.

Guo, D., and Z. Lu. 2000a. Mechanism of cGMP-gated channel block by intracellular polyamines. *J. Gen. Physiol*. 115:783–797.

Guo, D., and Z. Lu. 2000b. Mechanism of IRK1 channel block by intracellular polyamines. *J. Gen. Physiol*. 115:799–813.

Haghighi, A. P., and E. Cooper. 1998. Neuronal nicotinic acetylcholine receptors are blocked by intracellular spermine in a voltage dependent manner. *J. Neurosci*. 18:4050–4062.

Harris, A. L., D. C. Spray, and M. V. L. Bennett. 1981. Kinetic properties of a voltage-dependent junctional conductance. *J. Gen. Physiol*. 77:95–117.

Hoshi, T., W. N. Zagotta, and R. W. Aldrich. 1990. Biophysical and molecular mechanisms of *Shaker* potassium channel inactivation. *Science*. 250:533–538.

Hurst, R. S., R. Latorre, L. Toro, and E. Stefani. 1995. External barium block of *Shaker* potassium channels: evidence for two binding sites. *J. Gen. Physiol*. 106:1069–1087.

Imanaga, I., M. Kameyama, and H. Irisawa. 1987. Cell-to-cell diffusion of fluorescent dyes in paired ventricular myocytes. *Am. J. Physiol*. 252:H223–H232.

Imoto, K., C. Busch, B. Sakmann, M. Mishina, T. Konno, J. Nakai, H. Bujo, Y. Mori, K. Fukuda, and S. Numa. 1988. Rings of negatively charged amino acids determine the acetylcholine receptor conductance. *Nature*. 335:645–648.

Isacoff, E. Y., Y. N. Jan, and L. Y. Jan. 1991. Putative receptor for the cytoplasmic inactivation gate in the *Shaker* K^+ channel. *Nature*. 353:86–90.

Lee, J.-K., S. A. John, and J. N. Weiss. 1999. Novel gating mechanism of polyamine block in the strong inward rectifier K channel Kir2.1. *J. Gen. Physiol*. 113:555–563.

Lopatin, A. N., E. N. Makhina, and C. G. Nichols. 1994. Potassium channel block by cytoplasmic polyamines as the mechanism of intrinsic rectification. *Nature*. 372:366–369.

Lopatin, A. N., E. N. Makhina, and C. G. Nichols. 1995. The mechanism of inward rectification of potassium channels: "long-pore plugging" by cytoplasmic polyamines. *J. Gen. Physiol*. 106:923–955.

Lopatin, A. N., L. M. Shantz, C. A. Macintosh, C. G. Nichols, and A. E. Pegg. 2000. Modulation of potassium channels in the hearts of transgenic and mutant mice with altered polyamine biosynthesis. *J. Mol. Cell. Cardiol*. 32:2007–2024.

Lu, Z., and L. Ding. 1999. Blockade of a retinal cGMP-gated channel by polyamines. *J. Gen. Physiol*. 113:35–43.

MacKinnon, R., and G. Yellen. 1990. Mutations affecting TEA blockade and ion permeation in voltage-activated K^+ channels. *Science*. 250: 276–279.

Makowski, L., D. L. D. Casper, W. C. Phillips, and D. A. Goodenough. 1977. Gap junction structure II. Analysis of the X-ray diffraction data. *J. Cell Biol*. 74:629–645.

Manivannan, K., S. V. Ramanan, R. T. Mathias, and P. R. Brink. 1992. Multichannel recordings from membranes which contain gap junctions. *Biophys. J.* 61:216–227.

Musa, H., J. D. Gough, W. J. Lees, and R. D. Veenstra. 2001. Ionic blockade of the rat connexin40 gap junction channel by large tetraalkylammonium ions. *Biophys. J.* 81:3253–3274.

Nichols, C. G., E. N. Makhina, W. L. Pearson, Q. Sha, and A. N. Lopatin. 1996. Inward rectification and implications for cardiac excitability. *Circ. Res.* 78:1–7.

Oh, S., C. K. Abrams, V. K. Verselis, and T. A. Bargiello. 2000. Stoichiometry of transjunctional votlage-gating polarity reversal by a negative charge substitution in the amino terminus of a connexin32 chimera..*J. Gen. Physiol.* 116:13–31.

Perkins, G., D. Goodenough, and G. Sosinsky. 1997. Three-dimensional structure of the gap junction connexon. *Biophys. J.* 72:533–544.

Rock, D. M., and R. L. Macdonald. 1992. Spermine and related polyamines produce a voltage dependent reduction of N-methyl-D-aspartate receptor single-channel conductance. *Mol. Pharmacol.* 42:157–164.

Ruppersberg, J. P. 2000. Intracellular regulation of inward rectifier K^+ channels. *Pflügers Arch.* 441:1–11.

Scott, R. H., K. G. Sutton, and A. C. Dolphin. 1993. Interactions of polyamines with neuronal ion channels. *Trends Neurosci.* 16:153–160.

Shore, L., P. McLean, S. K. Gilmour, M. B. Hodgins, and M. E. Finbow. 2001. Polyamines regulate gap junction communication in connexin 43-expressing cells. *Biochem. J.* 357:489–495.

Spray, D. C., A. L. Harris, and M. V. L. Bennett. 1981. Equilibrium properties of a voltage dependent junctional conductance. *J. Gen. Physiol.* 77:77–93.

Trexler, E. B., M. V. L. Bennett, T. A. Bargiello, and V. K. Verselis. 1996. Voltage gating and permeation in a gap junction hemichannel. *Proc. Natl. Acad. Sci. USA.* 93:5836–5841.

Trexler, E. B., F. F. Bukauskas, J. Kronengold, T. A. Bargiello, and V. K. Verselis. 2000. Voltage gating and permeation in a gap junction hemichannel. *Biophys. J.* 79:3036–3051.

Unger, V. M., N. M. Kumar, N. B. Gilula, and M. Yeager. 1999. Three-dimensional structure of a recombinant gap junction membrane channel. *Science.* 283:1176–1180.

Valiunas, V., R. Weingart, and P. R. Brink. 2000. Formation of heterotypic gap junction channels by connexins 40 and 43. *Circ. Res.* 86:e42–e49.

Veenstra, R. D. 2000. Ion permeation through connexin gap junction channels: effects on conductance and selectivity. *In* Gap Junctions, Molecular Basis of Cell Communication in Health and Disease, Current Topics in Membranes, Vol. 49. C. Peracchia, editor. Academic Press, San Diego. 95–129.

Veenstra, R. D. 2001. Voltage clamp limitations of dual whole-cell gap junction current and voltage recordings. I. Conductance measurements. *Biophys. J.* 80:2231–2247.

Veenstra, R. D., H.-Z. Wang, D. A. Beblo, M. G. Chilton, A. L. Harris, E. C. Beyer, and P. R. Brink. 1995. Selectivity of connexin-specific gap junctions does not correlate with channel conductance. *Circ. Res.* 77:1156–1165.

Verselis, V., C. S. Ginter, and T. A. Bargiello. 1994. Opposite voltage gating polarities of two closely related connexins. *Nature.* 368:348–351.

Wang, H.-Z., J. Li, L. F. Lemanski, and R. D. Veenstra. 1992. Gating of mammalian gap junction channels by transjunctional voltage. *Biophys. J.* 63:139–151.

Wang, H.-Z., and R. D. Veenstra. 1997. Monovalent ion selectivity sequences of the rat connexin43 gap junction channel. *J. Gen. Physiol.* 109:491–507.

Wible, B. A., M. Taglialatela, E. Ficker, and A. M. Brown. 1994. Gating of inwardly rectifying K^+ channels localized to a single negatively charged residue. *Nature.* 371:246–249.

Williams, K. 1997. Interactions of polyamines with ion channels. *Biochem. J.* 325:289–297.

Woodhull, A. M. 1973. Ionic blockage of sodium channels in nerve. *J. Gen. Physiol.* 61:687–708.

Yang, J., Y. N. Jan, and L. Y. Jan. 1995. Control of rectification and permeation by residues in two distinct domains in an inward rectifier K^+ channel. *Neuron.* 14:1047–1054.

Yellen, G. 1987. Permeation in potassium channels: implications for channel structure. *Annu. Rev. Biophys. Biophys. Chem.* 16:227–246.

Zhou, X.-W., A. Pfahnl, R. Werner, A. Hudder, A. Llanes, A. Luebke, and G. Dahl. 1997. Identification of a pore lining segment in gap junction hemichannels. *Biophys. J.* 72:1946–1953.